A sequential optimization framework for simultaneous design variables selection and probability uncertainty allocation

Hai Fang[1], Chunlin Gong[1]✉, Chunna Li[1], Yunwei Zhang[1], Andrea Da Ronch[2]

Abstract In engineering design, the performance of system and the budget to control the uncertainty of design should be balanced, which means that it is better to select the design variable and allocate the size of uncertainty simultaneously. This work formulates this problem as an uncertainty optimization problem, where the input uncertainty is modeled by probability method and both the design variables and the uncertainty magnitude are included on the optimization variables. A sequence optimization framework is proposed to solve the optimization problem. Taylor-based first order method is used to translate the probability constraint into a deterministic constraint. A correction coefficient is calculated by dimensional adaptive polynomial chaos expansion method to improve the accuracy of the uncertainty analysis. The constraint translation and the correction coefficient calculation are executed sequentially. The accuracy and effectiveness of the proposed framework are validated by three benchmark problems, including a mathematical problem, a cantilever I-beam and a ten-bar truss case.

Keywords: uncertainty allocation, sequence optimization framework, Taylor-based uncertainty analysis, polynomial chaos expansion, dimensional adaptive sparse grid

1 Introduction

In engineering design, it is essential to understand and predict the range of acceptable disturbance variations in design parameters. There are many sources of uncertainty in design parameters, such as material properties, operation environment, manufacturing tolerances. In the case of a large disturbance, even small changes in the design parameters may have severe consequences on the required objective function value and the engineering system even may fail to operate. In recent years, the method of considering uncertainty in optimization design has drawn lots of interest, coined uncertainty optimization. Compared to the deterministic optimization, uncertainty optimization requires uncertainty analysis in the optimization process. The main uncertainty optimization problem is the Reliability-Based Design Optimization (RBDO).

The RBDO considers uncertainty in the constraint. Under the influence of uncertain design variables and system parameters, the constraint of a RBDO is the probability of meeting all the constraint functions, that is, the reliability constraint. Therefore, a RBDO method searches for the optimal values under reliability constraint (Aoues and Chateauneuf 2010; Lopez and Beck 2012; Meng et al. 2015,2015; Shahraki and Noorossana 2014; Silva et al. 2010; Torii et al. 2012; Valdebenito and Schueller 2010). In uncertainty optimization, quantifications of the reliability are needed. Primary methods used to determine the reliability metric include the First-Order Reliability Methods (FORM), the Second-Order Reliability Methods (SORM), the probability density evolution method (PDEM), Taylor-based method, the Gaussian quadrature, the stochastic expansion,

✉ Corresponding author: Chunlin Gong
leonwood@nwpu.edu.cn

1 Shaanxi Aerospace Flight Vehicle Design Key Laboratory, School of Astronautics, Northwestern Polytechnical University, Xi'an 710072, China

2 University of Southampton, Southampton, England, SO17 1BJ, United Kingdom

and the simulation-based methods (Li 2016; Park et al. 2015; Yang and Liu 2014); (Beyer and Sendhoff 2007; Keshavarzzadeh et al. 2016; Padulo et al. 2011; Schillings and Schulz 2015; Wu et al. 2018). Frequently used uncertainty optimization frameworks are derived from the FORM and the SORM. Based on the coupling between the uncertainty analysis and the optimization process, the uncertainty optimization methods can be divided into three groups: double loop approach (Keshtegar and Hao 2017; Meng et al. 2015; Youn et al. 2005), single-loop approach (Keshtegar and Hao 2016; Keshtegar and Hao 2018) and Sequential Optimization and Reliability Assessment (SORA) (Du and Chen 2004; Meng et al. 2016).

For RBDO, uncertain parameters or uncertain disturbances should be given, such as the standard variance of the input variables. However, the uncertain parameters for the preliminary design stage should be specified by designers, that is, the uncertainty allocation. Uncertainty allocation affects manufacturing costs and structural reliability. Generally speaking, large uncertainties that can be easily caused by simple processing will lead to performance degradation and difficulty in assembly, while small uncertainties require advanced manufacturing equipment and expensive manufacturing costs. Over the past few decades, many researchers have studied the uncertainty allocation problem, which optimizes the allocation of component tolerances to minimize total production costs and meet assembly requirements. The methods include early sequential quadratic programming-based methods (Chase et al. 1990), simulated annealing (Dupinet et al. 1996; Zhang and Wang 1993) Taguchi method (Kusiak and Feng 1995), genetic algorithms (Chen and Fischer 2000; Prabhaharan et al. 2004), and etc. Rao and Wu (Rao and Wu 2005) proposed an optimal allocation method based on interval analysis to determine the optimal values of mechanical assembly tolerances and clearances. Huang and Shiau (Huang and Shiau 2006) established a tolerance optimization model by using normal and lognormal distributions. Wu et al. (Wu et al. 2009) based on Monte Carlo simulations to allocate tolerances by minimizing the ratio between manufacturing costs and the probability of geometric requirements. Geetha et al. (Geetha et al. 2013) proposed a multi-objective optimization design to find the best tolerance allocation. However, in most existing studies, the design variables and uncertainty allocation are completely separated, so the optimal scheme of design variables and uncertainties allocation parameters cannot be found.

Hung and Chan (Hung and Chan 2013) added the cost regarding the tolerance to the objective function. Interval uncertainty is used to describe the tolerance, which consists of two parameters: the interval midpoint and the interval width. Jiang et al. (Jiang et al. 2014) considered tolerance allocation in interval uncertainty optimization, and proposed two methods by taking into account design variable tolerances to simultaneously optimize the basic size and tolerance of the design variables. The differences between the two methods are: the former is a multi-objective optimization method, taking into account the best performance and the least cost; the latter has only one objective function for the lowest cost, and the performance function is placed in the constraint to set the maximum allowable value. Luo and Liu et al. (Liu et al. 2016; Luo et al. 2015) considered the tolerance allocation method in the case of existing random disturbances in the model. For mixed uncertainties, a nested uncertainty analysis method was proposed, and a series approximation method was used to reduce the calculation amount. (Joseph 2016,2017) added the interval width parameter to the optimization to achieve the maximum interval allocation and transform the variables containing interval uncertainty into a first-order Taylor expansion into deterministic constraints.

With the above paragraphs as background, an uncertainty optimization model for simultaneous design variables selection and probability uncertainty allocation is here introduced as an extension of the optimization model proposed by Joseph (Joseph 2016,2017) and Jiang et al. (Jiang et al. 2014), in which the optimization problem is extended to the probability uncertainty problem. To solve this problem, the widely-used uncertainty optimization method SORA cannot be adopted directly because the uncertainty parameters are not explicitly presented in the optimization step. A

framework is proposed combining Taylor-based method, the PCE method, and the SORA framework to solve the problem.

The rest of the paper is organized as follows. In section 2, the formulation of the problem is described. In section 3, Taylor-based method and the PCE method are presented to deal with uncertainty analysis. The proposed framework is presented in section 3. Test cases are used to validate the effectiveness and accuracy of the framework in section 4. Finally, conclusions are given in section 5.

2 Problem statement

In reliability optimization, the uncertainty is modeled by the probability method, as shown in Fig.1. Therefore, the deterministic constraint is transformed into a reliability constraint, which is the constraint on the probability of limit state function in the safety domain or failure domain. The probability is a multidimensional integral of the limit state function. The probability in the safety domain can be expressed as:

$$\mathrm{P}\left\{\mathrm{g}(\mathbf{x}) \le 0\right\} = \int \cdots \int_{\mathrm{g}(\mathbf{x}) \le 0} \rho(\mathbf{x}) \mathrm{d}x_1 \mathrm{d}x_2 \cdots \mathrm{d}x_m . \tag{1}$$

where $\mathbf{x}$ is the uncertainty variable vector, m is the dimension of $\mathbf{x}$, x_i is the ith component of $\mathbf{x}$. The normal uncertainty widely used in uncertainty modeling is adopted in this paper. The normal uncertainty variable is expressed as $x_i \sim N\left(\bar{x}_i,\ \sigma_i^2\right)$, in which $\bar{x}_i$ is the mean value and σ_i is the standard deviation.

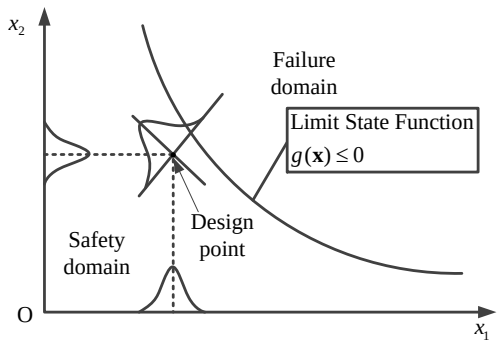

Fig.1 A two-dimensional uncertainty problem

The uncertainty optimization problem containing the deterministic variable vector $\mathbf{d}$ and the uncertainty variable vector $\mathbf{x}$ is described as Eq. (2).

$$\begin{aligned}
&\text{Given} && \boldsymbol{\sigma}_{\mathbf{x}} \\
&\text{find} && \mathbf{d}, \bar{\mathbf{x}} \\
&\min && f(\mathbf{d}, \mathbf{x}) \\
&\text{s.t.} && \mathrm{P}\left\{g_i(\mathbf{d}, \mathbf{x}) \le 0\right\} \le R_i, i = 1,2,\ldots,\ n_g \\
& && \mathbf{d}_{\mathrm{L}},, \mathbf{d},, \mathbf{d}_{\mathrm{R}}, \bar{\mathbf{x}}^{\mathrm{L}},, \bar{\mathbf{x}},, \bar{\mathbf{x}}^{\mathrm{R}} \\
& && x_j \sim N\left(\bar{x}_j,\ \sigma_{x_j}^{\ 2}\right),\ j = 1,2,\ldots,\ m
\end{aligned} \tag{2}$$

where, R_i is the reliability requirement on the inequality constraint, $\bar{\mathbf{x}}$ is the mean value vector, $\boldsymbol{\sigma}_{\mathbf{x}}$ is the standard deviation. The subscripts L and R represent, respectively, the lower and upper bounds. For the uncertainty in the objective function, a new variable $\prime$ and a new constraint are introduced, as shown in Eq. (3).

$$
\begin{aligned}
&\text{Given} && \boldsymbol{\sigma}_{\mathbf{x}} \\
&\text{find} && \mathbf{d}, \bar{\mathbf{x}} \\
&\min && \nu \\
&\text{s.t.} && \mathrm{P}\left\{g_i(\mathbf{d},\mathbf{x}) \le 0\right\} \le R_i, i = 1,2,\ldots,\ n_g \\
& && \mathrm{P}\left\{f(\mathbf{d},\mathbf{x}) - \nu \le 0\right\} \le R_f \\
& && \mathbf{d}_{\mathrm{L}},, \mathbf{d},, \mathbf{d}_{\mathrm{R}}, \bar{\mathbf{x}}^{\mathrm{L}},, \bar{\mathbf{x}},, \bar{\mathbf{x}}^{\mathrm{R}} \\
& && x_j \sim N\left(\bar{x}_j,\ \sigma_{x_j}{}^2\right),\ j = 1,2,\ldots,\ m
\end{aligned}
\tag{3}
$$

In Eq. (3), the standard deviation shall be specified. However, for the preliminary design stage, $\boldsymbol{\sigma}_{\mathbf{x}}$ is unknown when the uncertainty is not allocated. As a result, it is necessary to add uncertainty allocation to the problem, which can be further expressed as in Eq. (4). Generally, reducing the standard deviation will lead to an increase in the uncertainty control cost.

$$
\begin{aligned}
&\text{Find} && \mathbf{d}, \bar{\mathbf{x}}, \boldsymbol{\sigma}_{\mathbf{x}} \\
&\min && \left[\nu, \mathrm{cost}\left(\boldsymbol{\sigma}_{\mathbf{x}}\right)\right] \\
&\text{s.t.} && \mathrm{P}\left\{g(\mathbf{d},\mathbf{x}) \le 0\right\} \le R_i, i = 1,2,\ldots,\ ng \\
& && \mathrm{P}\left\{f(\mathbf{d},\mathbf{x}) - \nu \le 0\right\} \le R_f \\
& && x_{\mathrm{aj}} \sim N\left(\bar{x}_j,\ \sigma_{x_j}{}^2\right),\ j = 1,2,\ldots,\ m \\
& && \mathbf{d}_{\mathrm{L}},, \mathbf{d},, \mathbf{d}_{\mathrm{R}}, \bar{\mathbf{x}}^{\mathrm{L}},, \bar{\mathbf{x}},, \bar{\mathbf{x}}^{\mathrm{R}}, \boldsymbol{\sigma}_{\mathbf{x}}{}^{\mathrm{L}},, \boldsymbol{\sigma}_{\mathbf{x}},, \boldsymbol{\sigma}_{\mathbf{x}}{}^{\mathrm{R}}
\end{aligned}
\tag{4}
$$

The weighted coefficient method is adopted to transform the multi-objective optimization problem into a singular objective optimization problem, as reported in Eq. (5). In this paper, the cost induced by reducing the standard deviation is simply modeled as $f_{\mathrm{rob}} = \sum \omega_j \psi_j$, and $\boldsymbol{\omega}$ is a weighting vector (Joseph 2016,2017).

$$
\begin{aligned}
&\text{find} && \mathbf{d}, \bar{\mathbf{x}}, \boldsymbol{\psi} \\
&\min && J = \alpha f_{\mathrm{opt}} + (\alpha - 1) f_{\mathrm{rob}} \\
&\text{s.t.} && \mathrm{P}\left\{g(\mathbf{d},\mathbf{x}) \le 0\right\} \le R_i, i = 1,2,\ldots,\ ng \\
& && \mathrm{P}\left\{f(\mathbf{d},\mathbf{x}) - \nu \le 0\right\} \le R_f \\
& && x_j \sim N\left(\bar{x}_j,\ \sigma_{x_j}{}^2\right),\ \psi_j = \sigma_{x_j} / \bar{x}_j,\ j = 1,2,\ldots,\ m \\
& && \mathbf{d}_{\mathrm{L}},, \mathbf{d},, \mathbf{d}_{\mathrm{R}}, \bar{\mathbf{x}}^{\mathrm{L}},, \bar{\mathbf{x}},, \bar{\mathbf{x}}^{\mathrm{R}}, \boldsymbol{\psi}_{\mathrm{L}},, \boldsymbol{\psi},, \boldsymbol{\psi}_{\mathrm{R}} \\
&\text{where} && f_{\mathrm{opt}} = \nu / \beta - 1,\ f_{\mathrm{rob}} = \sum \omega_j \psi_j
\end{aligned}
\tag{5}
$$

where β is the objective function value of the deterministic optimization solution. α is the coefficient that combines the two objectives, and its value is constrained as $0 < \alpha < 1.0$. When α increases, the weight coefficient of f_{opt} increases and the weight coefficient of the f_{rob} decreases, which leads to smaller standard deviation and γ will be closer to the deterministic optimization value β.

3 The uncertainty analysis methods

Equation (1) shows that the probability result is a multi-dimensional integral, and this can be solved by numerical integration or the Monte Carlo Simulation (MCS) method. However, the system model cannot be expressed explicitly, and the calculation of the model may incur in large computing costs because a large number of calculations need to be computed by the numerical integration or the MCS method. Therefore, several approximate methods for uncertainty analysis have been proposed. The uncertainty analysis method based on the first-order Taylor series expansion has an advantage in efficiency, while it may lead to low accuracy for nonlinear problems.

Uncertainty analysis based on dimensional adaptive polynomial chaos expansion has an advantage in accuracy, but requires more model calculations in comparison with the methods based on the first-order Taylor series expansion. This paper combines the two methods to construct a probability uncertainty optimization method based on margin correction.

3.1 Uncertainty analysis based on first-order approximation

3.1.1 Probabilistic moment analysis ~~based on first-order approximation~~

Taylor expansion method can be used to analyze the low-order moment information of the system response under the influence of random uncertainty. To calculate the moment information of the system model, $g(\mathbf{x})$, at point $\mathbf{x}_0$, the first-order Taylor expansion around point $\mathbf{x}_0$ is expressed

$$g(\mathbf{x}) \approx g(\mathbf{x}_0) + \sum_{i=1}^{n_x} \frac{\partial g(\mathbf{x}_0)}{\partial x_i}(x_i - x_{i0}) \tag{6}$$

where, x_i and x_{i0} are the ith component of $\mathbf{x}$ and $\mathbf{x}_0$, respectively. Based on Taylor expansion, the mean, μ_g, and the standard deviation, σ_g, of the system output at point $\mathbf{x}_0$ are expressed by

$$\begin{cases} \mu_g \approx g(\mathbf{x}_0) + \sum_{i=1}^{m} \frac{\partial g(\mathbf{x}_0)}{\partial x_i} E(x_i - x_{i0}) \\ \sigma_g \approx \sqrt{\sum_{i=1}^{m} \left(\frac{\partial g(\mathbf{x}_0)}{\partial x_i} \right)^2 \sigma_{x_i}^2 + 2 \sum_{i=1}^{m} \sum_{j=1+1}^{m} \frac{\partial g(\mathbf{x}_0)}{\partial x_i} \frac{\partial g(\mathbf{x}_0)}{\partial x_j} \operatorname{cov}(x_i, x_j)} \end{cases} \tag{7}$$

$\operatorname{cov}(x_i, x_j)$ is the correlation coefficient between the uncertainty variables, x_i and x_j. If the input variables are uncorrelated, then the second-order information can be ignored, and the approximated mean and standard deviation of the system output are

$$\begin{cases} \mu_g \approx g(\mathbf{x}_0) \\ \sigma_g \approx \sqrt{\sum_{i=1}^{n_x} \left(\frac{\partial g(\mathbf{x}_0)}{\partial x_i} \right)^2 \sigma_{x_i}^2} \end{cases} \tag{8}$$

This analysis method is efficient, and convenient for calculation and application, but it also has some limitations. Since the method is based on the first-order expansion, the variances of the uncertainty variables should not be too large, as well as the nonlinearity degree of the system model, otherwise, the calculation accuracy will be greatly affected.

3.1.2 Moment matching method

Taylor series expansion-based method can be used to calculate the mean and variance of the model output. To deal with the uncertainty constraints in Eq.(5), the moment matching method is used. Assume that the output $g(\mathbf{x})$ is normally distributed, then $(g(\mathbf{x}) - \mu_g)/\sigma_g$ follows the standard normal distribution. The probability of $g(\mathbf{x}) \le 0$ can be formulated as

$$\mathrm{P}\{g(\mathbf{x}) \le 0\} = \Phi\left(-\frac{\mu_g}{\sigma_g}\right) \tag{9}$$

in which Φ is the cumulative distribution function of the standard normal distribution, given by

$$\Phi(x)=\frac{1}{\sqrt{2\pi}}\int_{-\infty}^{x}e^{\left(-x^2/2\right)}dx \tag{10}$$

Finally, the probability constraints is equivalent to

$$\mu_g+\Phi^{-1}(R)\sigma_g\le 0 \tag{11}$$

where $R=\Pr\{g(\mathbf{x})\le 0\}$ is the probability or reliability requirement to the inequality constraint.

3.1.3 The shifted constraint

Combining the first-order approximation and the moment matching method, the probability constraints are reformulated

$$g\left(\mathbf{x}\right)+\Phi^{-1}(R)\sqrt{\sum_{i=1}^{m}\left(\frac{\partial g\left(\mathbf{x}\right)}{\partial x_i}\right)^2\sigma_{x_i}^2}\le 0\cdot \tag{12}$$

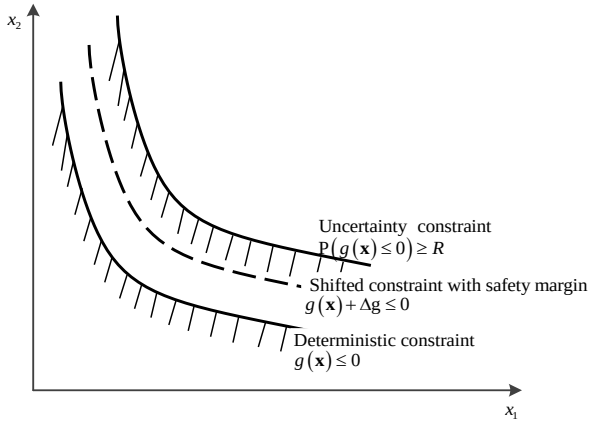

Fig.2 The shifted constraint with Δg

As shown in Eq. (12) and Fig.2, a safety margin is added to the deterministic constraint:

$$\Delta g=\Phi^{-1}(R)\sqrt{\sum_{i=1}^{m}\left(\frac{\partial g\left(\mathbf{x}\right)}{\partial x_i}\right)^2\sigma_{x_i}^2}\cdot \tag{13}$$

The method based on first-order Taylor expansion and probability distribution moment matching includes first-order approximation and output normal distribution assumptions. Therefore, the safety margin in Eq.(13) needs to be modified to improve the accuracy. In this paper, a method based on dimensional adaptive polynomial chaos expansion (PCE) is adopted to modify the first-order method during the optimization design process.

3.2 Uncertainty analysis based on the dimensional adaptive polynomial chaos expansion method

3.2.1 Non-intrusive PCE

The PCE is based on multidimensional orthogonal polynomial approximation and has been widely used in reliability quantization. (Keshavarzzadeh et al. 2016; Papadimitriou and Papadimitriou 2016; Schillings and Schulz 2015; Torii et al. 2017) The PCE of $g(\mathbf{d},\mathbf{x})$ is written (Schillings 2010).

$$g(\mathbf{d},\mathbf{x}) = \sum_{j=0}^{\infty} \sum_{\mathbf{i}\in\{\|\mathbf{i}\|_1 = j\}} \tilde{g}_{\mathbf{i}}(\mathbf{d}) \cdot B_{\mathbf{i}}(\mathbf{x}) \tag{14}$$

where $\mathbf{x}$ is a random vector with dim random variables, $\|\mathbf{i}\|_1 = \sum_{j=1}^{dim} i_j$ is the l_1 norm of the index vector, $\tilde{g}_{\mathbf{i}}(\mathbf{d})$ is the deterministic coefficients, $B_{\mathbf{i}}(\mathbf{x})$ is the polynomial bases determined by the Wiener-Askey scheme (Xiu and Karniadakis 2002). The Hermite orthogonal polynomial is adopted to simulate the effects of continuous random variables with normalized probability distributions. In practice, the infinite extension is truncated by a finite number, while the $p-$order truncation expansion is represented in the term-based form in Eq.(15)

$$\begin{aligned} g(\mathbf{d},\mathbf{x}) &= \sum_{i=0}^{n_{pc}} \tilde{g}_i(\mathbf{d}) \cdot \Psi_i(\mathbf{x}), \\ \{\Psi_i(\mathbf{x})\}_{i=0}^{n_{pc}} &\equiv \left\{ B_{\mathbf{i}}(\mathbf{x}) \right\}_{\|\mathbf{i}\|_1 = 0}^{p} \end{aligned} \tag{15}$$

where $n_{pc} = (s+p)!/(s!p!) - 1$ is the number of expansion terms, s is the number of random variables.

The PCE separates $g(\mathbf{d},\mathbf{x})$ into a determination portion $\tilde{g}_i(\mathbf{d})$ and the random portion $\Psi_i(\mathbf{x}(\omega))$, as shown in Eq. (15). The non-intrusive method that uses the simulation code as a black-box is adopted to calculate $\tilde{g}_i(\mathbf{d})$. Considering the orthogonal characteristics with respect to PDF $\rho(\mathbf{x})$, $\tilde{g}_i(\mathbf{d})$ is evaluated using the projection method

$$\tilde{g}_i(d) = \frac{\int_{\Omega} g(\mathbf{d},\mathbf{x}) \Psi_i(\mathbf{x}) \rho(\mathbf{x}) d\mathbf{x}}{\int_{\Omega} \left[\Psi_i(\mathbf{x})\right]^2 \rho(\mathbf{x}) d\mathbf{x}} \tag{16}$$

After obtaining the PCE coefficients, by using the PCE instead of the original function to evaluate the statistics, the R percentile can be solved using (Du and Chen 2004)

$$R = P\{g(\mathbf{d},\mathbf{x}) \le g^R\} \approx \int_{g(\mathbf{x})\le 0} \sum_{i=0}^{n_{PC}} \tilde{g}_i(\mathbf{d}) \cdot \Psi_i(\mathbf{x}) \rho(\mathbf{x}) d\mathbf{x} \tag{17}$$

As shown in Fig.3, a safety margin Δg based on the R percentile is defined

$$\Delta g = g^R - g(\mathbf{d},\bar{\mathbf{x}}) \tag{18}$$

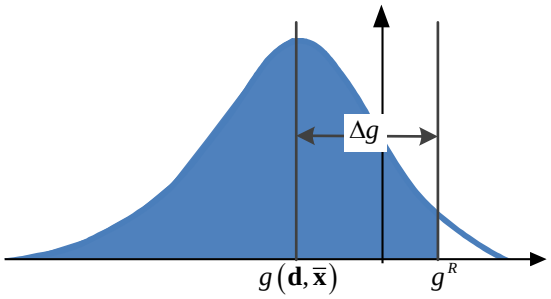

Fig.3 R percentile and safety margin of $g(\mathbf{d},\mathbf{x})$

To obtain the R percentile, the distribution of the output is needed. As is stated in the last section, the output distribution and the corresponding R percentile can be obtained by using the Monte Carlo Simulation (MCS) on the PCE.

Further, the dimensional adaptive sparse grid method is introduced to discretize the probabilistic space method and to evaluate the multi-dimensional integral in Eq.(16).

3.2.2 **Dimensional adaptive sparse grid**

The full tensor grid method using tensor products of one-dimensional quadrature rules is the most straightforward general technique for multidimensional integration. However, the method leads to an exponential growth of function evaluations as the dimension increases, which is called the curse of dimensionality (Da Ronch et al. 2011). To overcome such difficulty, Smoljak (1963) developed the sparse grid method. With $k \geq dim$, the sparse grid integral is caldulated by Eq. (19).

$$S(k,dim) = \sum_{k-dim+1 \leq \|\mathbf{i}\|_1 \leq k} (-1)^{k-\|\mathbf{i}\|_1} \cdot \binom{dim-1}{k-\|\mathbf{i}\|_1} \cdot (Q^{i_1} \otimes Q^{i_2} \otimes \cdots \otimes Q^{i_{dim}}) \tag{19}$$

in which Q^i is a sequence of univariate quadrature formulas and the corresponding quadrature order is exact for polynomials up to order i. Considering a function with bounded mixed derivative up to order k, the error bound of the sparse grid with N grid points is $O(N^{-k} \cdot (\log N)^{(k+1)(d-1)})$, while the error range of the full tensor grid with N grid points is $O\left(N^{-k/d}\right)$. (Schillings 2010). Therefore, the sparse grid method can overcome the curse of dimensionality and is suitable for dealing with high-dimensional integration problems.

With $Q^0 = 0$, a difference formula $\Delta^i = Q^{i+1} - Q^i$ can be defined using the nested rules. Therefore, the sparse grid method can be expressed in incremental form as

$$S(k,dim) = S(k-1,dim) + \sum_{\|\mathbf{i}\|_1 = k} \Delta^{i_1} \otimes \Delta^{i_2} \otimes \cdots \otimes \Delta^{i_{dim}} \tag{20}$$

Based on the incremental form, the dimensional adaptive sparse grid starts from a coarse sparse grid, then adds grid points sequentially according to the importance of each dimension. The sparse grid integral with the multi-index set $\mathbf{I} = \{\mathbf{i} : k - dim + 1 \leq \|\mathbf{i}\|_1 \leq k\}$ is :

$$S(k,dim) = \sum_{\mathbf{i} \in \mathbf{I}} \Delta^{i_1} \otimes \Delta^{i_2} \otimes \cdots \otimes \Delta^{i_{dim}} . \tag{21}$$

A forward neighborhood set of $\mathbf{I}$ is defined as

$$\mathbf{I}_{\text{nei}} = \{\mathbf{i}_{\text{nei}} : \mathbf{i}_{\text{nei}} = \mathbf{i} + \mathbf{e}_j, \mathbf{i}_{\text{nei}} - \mathbf{e}_k \in \mathbf{I}, \mathbf{i} \in \mathbf{I}, 1 \leq j \leq dim, 1 \leq k \leq dim\} . \tag{22}$$

Using the grid points identified by the sparse grid with the multi-index set $\mathbf{I}$, the PCE coefficients can be evaluated by Eq. (16), and the PCE is constructed as Eq. (15). The output distribution is obtained using the MCS on the PCE, and a safety margin is solved based on Eq. (17) and Eq. (18). For a multi-index $\mathbf{i}_{\text{nei}} \in \mathbf{I}_{\text{nei}}$, an error indicator is defined

$$\delta_{\mathbf{i}_{\text{nei}}} = \Delta g^{\mathbf{I} + \{\mathbf{i}_{\text{nei}}\}} - \Delta g^{\mathbf{I}} \tag{23}$$

The multi-index $\mathbf{i}_{\text{nei}}$ that induces the maximum $\delta_{\mathbf{i}_{\text{nei}}}$ is added to the multi-index set, and the corresponding grid points are added to the sparse grid until the maximum $\delta_{\mathbf{i}_{\text{nei}}}$ is less than the required error limit. Therefore, the PCE constructing the dimensional adaptive sparse grid is problem dependent, which can reduce the number of function evaluations.

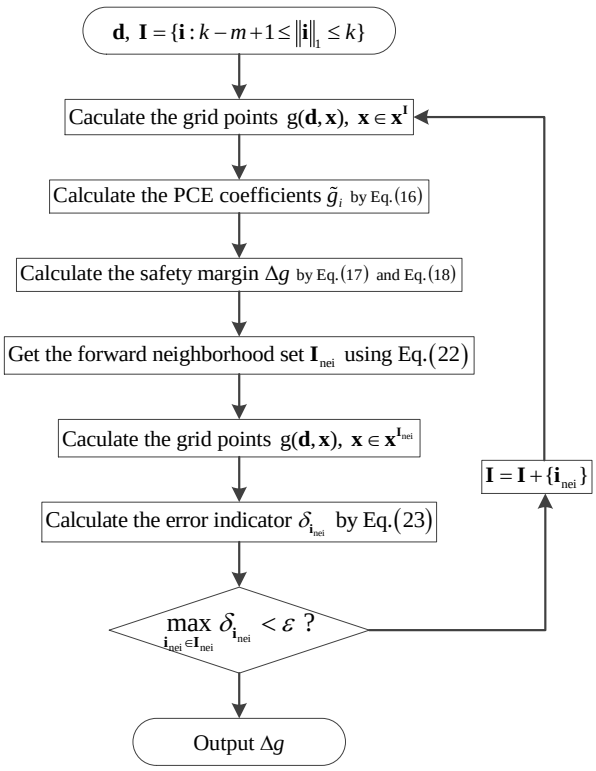

Fig.4 Calculation of safety margin based on dimensional adaptive polynomial chaos expansion

The non-intrusive polynomial chaos expansion method and the dimensional adaptive sparse grid method are used to construct a dimensional adaptive polynomial expansion method for solving the safety margin. Define the initial multi-index set as $\mathbf{I}=\{\mathbf{i}:k-m+1\le\|\mathbf{i}\|_1\le k\}$, and generate a sparse grid, then set the error limit ε. The safety margin is calculated based on dimensional adaptive polynomial chaos expansion is shown in Fig.4.

4 Sequential optimization based on margin correction

4.1 The sequential optimization and reliability assessment method

The Sequential Optimization and Reliability Assessment (SORA) as shown in Fig.5 is widely used in solving uncertainty optimization problems (Du and Chen 2004; Yi et al. 2016). The main idea is to decouple the uncertainty analysis from the outer optimization search, and to execute the optimization search and uncertainty analysis sequentially. In the sequential optimization process, based on the information obtained from the uncertainty analysis in the previous step, the probability constraint is converted into an equivalent deterministic constraint. After finishing the deterministic optimization, an uncertainty analysis is performed on the obtained optimal solution, then the analysis results are used to guide the next deterministic optimization. The SORA method has a simple structure and is easy to deploy.

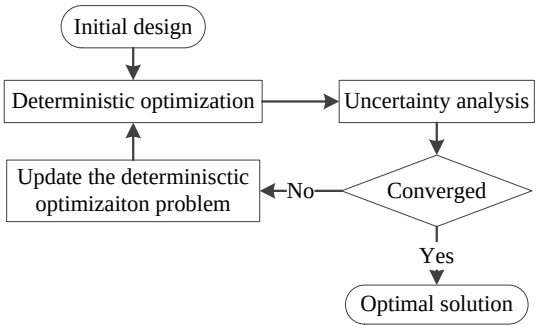

Fig.5 Flowchart of the SORA method

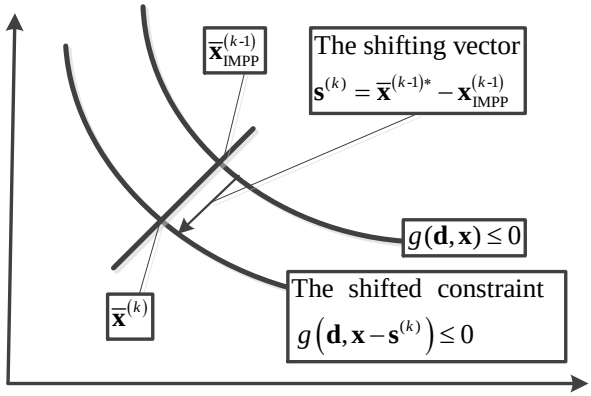

Fig.6 The shifted constraint of SORA

The probability constraint is converted into a deterministic constraint using the inverse most probable point (IMPP), as shown in Fig.6. The IMPP is the point that minimizes the limit state function subjected to the prescribed reliability constraint in the U-space (Du and Chen 2004; Li et al. 2019). It can be obtained by solving the minimization problem

$$\begin{cases} \min & g(\mathbf{u}) \\ \text{s.t.} & \left(\mathbf{u}^T\mathbf{u}\right)^{1/2} = \Phi^{-1}(R) \end{cases} \tag{24}$$

where $u_i = \Phi^{-1}\left(\text{CDF}_{x_i}\left(x_i\right)\right), i = 1,2,\ldots,m$ are standard normal distribution variables, and $\text{CDF}_{x_i}\left(x_i\right)$ is the cumulative distribution function of x_i .

The optimal solution of the (k-1)-th deterministic optimization problem is donated as $\bar{\mathbf{x}}^{(k-1)*}$, and the corresponding constraint function reliability index requires that the IMPP is $\mathbf{u}_{\text{IMPP}}^{(k-1)}$, then the ($k$+1)-th deterministic optimization problem can be expressed as Eq. (25).

$$\begin{aligned} &\text{Given} && \bar{\mathbf{x}}^{(k-1)*}, \mathbf{x}_{\text{IMPP}}^{(k-1)} \\ &\text{find} && \mathbf{d}, \bar{\mathbf{x}} \\ &\min && f\left(\mathbf{d}, \bar{\mathbf{x}}\right) \\ &\text{s.t.} && \text{g}\left(\mathbf{d}, \bar{\mathbf{x}} - \mathbf{s}^{(k)}\right) \le 0 \\ & && \mathbf{s}^{(k)} = \bar{\mathbf{x}}^{(k-1)*} - \mathbf{x}_{\text{IMPP}}^{(k-1)} \end{aligned} \tag{25}$$

There is no standard deviation term in the deterministic optimization of Eq. (25), as the standard deviation term cannot affect the optimization process. Therefore, the SORA method cannot be directly applied to the uncertainty optimization for simultaneous design variables selection and probability uncertainty allocation because the standard deviation is not explicitly presented in Eq. (25). The sequential idea of SORA which separates the uncertainty optimization into the

deterministic optimization and uncertainty analysis is adopted in the proposed framework.

4.2 Proposed framework based on margin correction

Based on the first-order approximation method and the dimensional adaptive polynomial chaos expansion method, the margin correction coefficient is defined as

$$\gamma = \frac{g^R - \mathrm{g}(\mathbf{d}, \bar{\mathbf{x}})}{\Phi^{-1}(R)\left(\sum_{i=1}^{m}\left|\frac{\partial \mathrm{g}(\mathbf{d}, \bar{\mathbf{x}})}{\partial x_i}\sigma_{x_i}\right|\right)} \tag{26}$$

where g^R is solved by the dimensional adaptive polynomial chaos expansion method. The numerator is the safety margin solved by the polynomial chaos method, and the denominator is the safety margin solved by the first-order approximate method. Therefore, the margin correction coefficient can be used to modify the first-order approximate method in the optimization process. In combination with the optimization design model considering the margin correction coefficient and the sequential optimization solution, an optimization design process with the uncertainty allocation based on the margin correction is constructed, as is shown in Fig.7. The whole process is divided into two steps: deterministic optimization and uncertainty optimization.

- Step 1. Deterministic optimization

As shown in Fig.7, the uncertainty is ignored in the deterministic optimization step, in which the variable is the mean of the uncertainty variable. The objective of the optimal solution is passed to the uncertainty optimization step, which is used to normalize the objective function of the uncertain optimization. Furthermore, the optimal solution of the deterministic optimization can be used as the initial solution of uncertainty optimization.

- Step 2. Uncertainty optimization

In the simultaneous design variables selection and probability uncertainty allocation, two sets of weighting coefficients α and ω_i are used to construct a single objective function. Therefore, a single-objective optimization algorithm can be used to solve the optimization problem, such as the gradient-based algorithm, the genetic algorithm, etc. Because the uncertainty optimization searches within the bounds of the deterministic optimization, the efficient gradient-based local search optimization algorithm is selected to improve the solution efficiency.

Analogous SORA converts uncertainty optimization into sequential execution of a two-step process with the shifted deterministic optimization and uncertainty analysis. The optimization design process proposed in this paper also includes two steps: the uncertainty optimization based on the modified first-order approximation method, and correction coefficients evaluation based on dimensional adaptive polynomial chaos expansion.

- Step 2.1 Uncertainty optimization based on the modified first-order approximation method

Unlike shifted deterministic optimization of the SORA, the uncertainty optimization of the modified first-order approximation method explicitly includes the standard deviation term in the safety margin, which can consider the influence of the standard deviation term in the optimization search. Due to the first-order approximation and normal distribution assumptions contained in the first-order approximation method, there will be an error in the safety margin for the nonlinear function and the abnormal distribution output. This paper uses a correction coefficient to modify the first-order approximation method, and adjusts the correction coefficient in the optimization process to finally reach convergence.

- Step 2.2 Correction coefficient evaluation based on dimensional adaptive polynomial chaos expansion

The process of solving the safety margin based on the adaptive polynomial chaos method is shown in Fig.4. This method is a high-order method, which has the advantage of high accuracy in

comparison with the first-order approximation method.

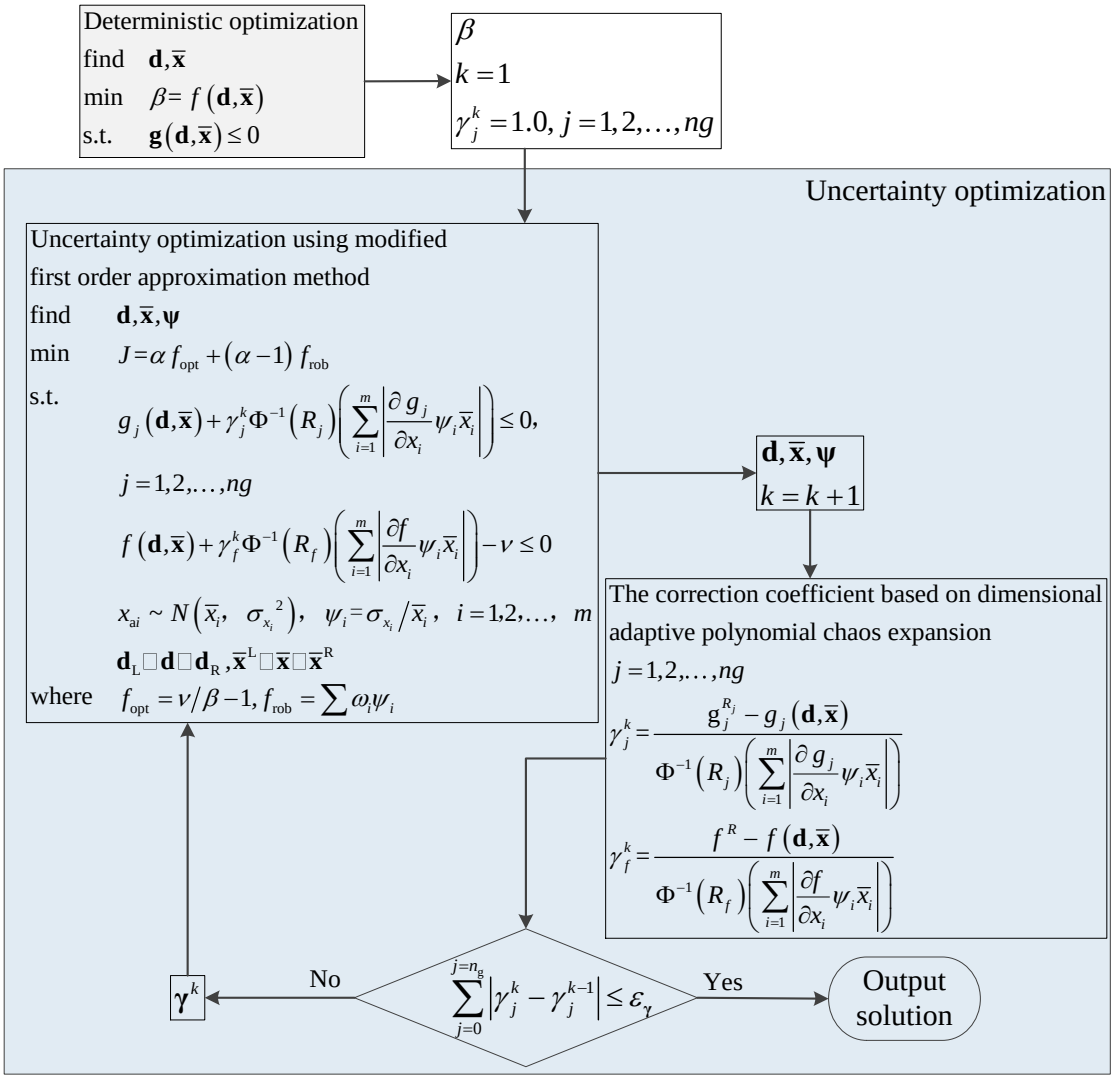

Fig.7 The proposed framework based on the safety margin correction

To accelerate convergence, the search interval is adjusted in the optimization design process. In this paper, the search interval reduction method is implemented, and the adjustment rules are

$$\begin{aligned} d_{i,\mathrm{L}}^k &= \max\left(d_{i,*}^{k-1} - \left(d_{i,*}^{k-1} - x_{i,\mathrm{L}}^0\right)q_i^k \ ,\ d_{i,\mathrm{L}}^0\right) \\ d_{i,\mathrm{R}}^k &= \min\left(d_{i,*}^{k-1} + \left(d_{i,\mathrm{R}}^0 - x_{i,*}^{k-1}\right)q_i^k \ ,\ d_{i,\mathrm{R}}^0\right) \end{aligned} \tag{27}$$

where, $d_{i,\mathrm{L}}^0$ and $d_{i,\mathrm{R}}^0$ are the initial upper and lower bounds of d_i , respectively. $d_{i,*}^{k-1}$ is the optimal solution of the $(k-1)$ cycle. $d_{i,\mathrm{L}}^k$ and $d_{i,\mathrm{R}}^k$ are the upper and lower bounds of d_i in the k cycle, respectively. q_i^k is the reduction coefficient for the *i*-th variable in the k -th cycle. Because the optimization solution of each cycle in the uncertainty optimization process of the modified first-order approximation method changes with the correction coefficient, the reduction coefficient is selected based on the maximum relative error of the correction coefficient. The maximum value of the correction coefficient error can be solved as Eq. (28).

$$\delta_\gamma^{k,\max} = \max\left\{\delta_\gamma \,\middle|\, \delta_\gamma = \left|\left(\gamma_j^{k-1} - \gamma_j^{k-2}\right)/\gamma_j^{k-1}\right|, j=1,2,\ldots,ng\right\} \tag{28}$$

Therefore, the reduction coefficient becomes

$$q^k=\begin{cases}2q^{k-1} & \delta_\gamma^{k,\max}\geq 0.75\\ q^{k-1} & 0.25<\delta_\gamma^{k,\max}<0.75\\ 0.5q^{k-1} & \delta_\gamma^{k,\max}\leq\ 0.25\end{cases} \tag{29}$$

In next section, the proposed method is validated by several examples.

5 Examples and discussion

5.1 Mathematical example

The mathematical example given in Eq. (30) is referenced from the literature (Joseph, 2017). The example contains two nonlinear constraints and a nonlinear objective function. It may represent optimization problems in mechanical design applications.

$$\begin{aligned}&\text{Find} && \{x_1,x_2\}\\ &\min && f=2x_1+21x_2-x_1x_2+100\\ &\text{s.t.} && \mathrm{g}_1=3(x_1-15)^2+(x_2-20)^2-220\leq 0\\ & && \mathrm{g}_2=x_1x_2+12x_2-430\leq 0\\ & && 10\leq x_1\leq 25, 5\leq x_2\leq 15\end{aligned} \tag{30}$$

The optimal solution of the deterministic optimization problem is x_1 =22.3894, x_2 =12.5039, f =127.4063. The simultaneous design variables selection and probability uncertainty allocation model of the above problem is formulated as Eq. (31).

$$\begin{aligned}&\text{find} && \{\bar{x}_{\mathrm{a}1},\bar{x}_{\mathrm{a}2},\nu,\psi_1,\psi_2\}\\ &\min && J=\alpha f_{\mathrm{opt}}+(\alpha-1)f_{\mathrm{rob}}\\ &\text{s.t.} && \mathrm{P}\{g_j(x_{\mathrm{a}1},x_{\mathrm{a}2})\leq 0\}\geq 0.98,\ j=1,2\\ & && \mathrm{P}\{f(x_{\mathrm{a}1},x_{\mathrm{a}2})\leq\nu\}\geq 0.98\\ & && x_{ai}\sim N(\bar{x}_{ai},\ \sigma_{x_{ai}}{}^2),\ \psi_i=\sigma_{x_{ai}}/\bar{x}_{ai},\ i=1,2\\ &\text{where} && f_{\mathrm{opt}}=\nu/\beta-1, \mathrm{f}_{\mathrm{rob}}=\sum\omega_i\psi_i\end{aligned} \tag{31}$$

According to the proposed framework in Fig.7, the uncertainty optimization based on the modified first-order approximation method is as expressed as Eq. (32).。

$$\begin{aligned}&\min && J=\alpha f_{\mathrm{opt}}+(\alpha-1.0)f_{\mathrm{rob}}\\ &\text{w.r.t.} && \{\bar{x}_{\mathrm{a}1},\bar{x}_{\mathrm{a}2},\ \psi_1,\ \psi_2,\ \nu\}\\ &\text{s.t.} && \mathrm{g}_j(\mathbf{d},\bar{\mathbf{x}}_{\mathrm{a}})+\gamma_j\Phi^{-1}(0.98)\left(\sum_{i=1}^{2}\left|\frac{\partial \mathrm{g}_j}{\partial x_{ai}}\psi_i\bar{x}_{ai}\right|\right)\leq 0,\ j=1,2\\ & && f(\mathbf{d},\bar{\mathbf{x}}_{\mathrm{a}})+\gamma_3\Phi^{-1}(0.98)\left(\sum_{i=1}^{2}\left|\frac{\partial f}{\partial x_{ai}}\psi_i\bar{x}_{ai}\right|\right)-\nu\leq 0\\ & && 10.0^{-5}\ \leq\psi_i\leq 0.1,\ i=1,2\\ &\text{where} && f_{\mathrm{opt}}=\nu/127.406\text{-}1, f_{\mathrm{rob}}=(\omega_1\psi_1+\omega_2\psi_2)\end{aligned} \tag{32}$$

where, Φ^{-1} is the reverse function of the standard normal cumulative distribution function, and $\Phi^{-1}(0.98)=2.0537$. The correction coefficient is calculated using Eq. (26). The weighted coefficients of the standard deviations are set to $\omega_1=\omega_2=0.5$. Fig.8 shows the correction coefficients and the optimization solutions with respect to different α .

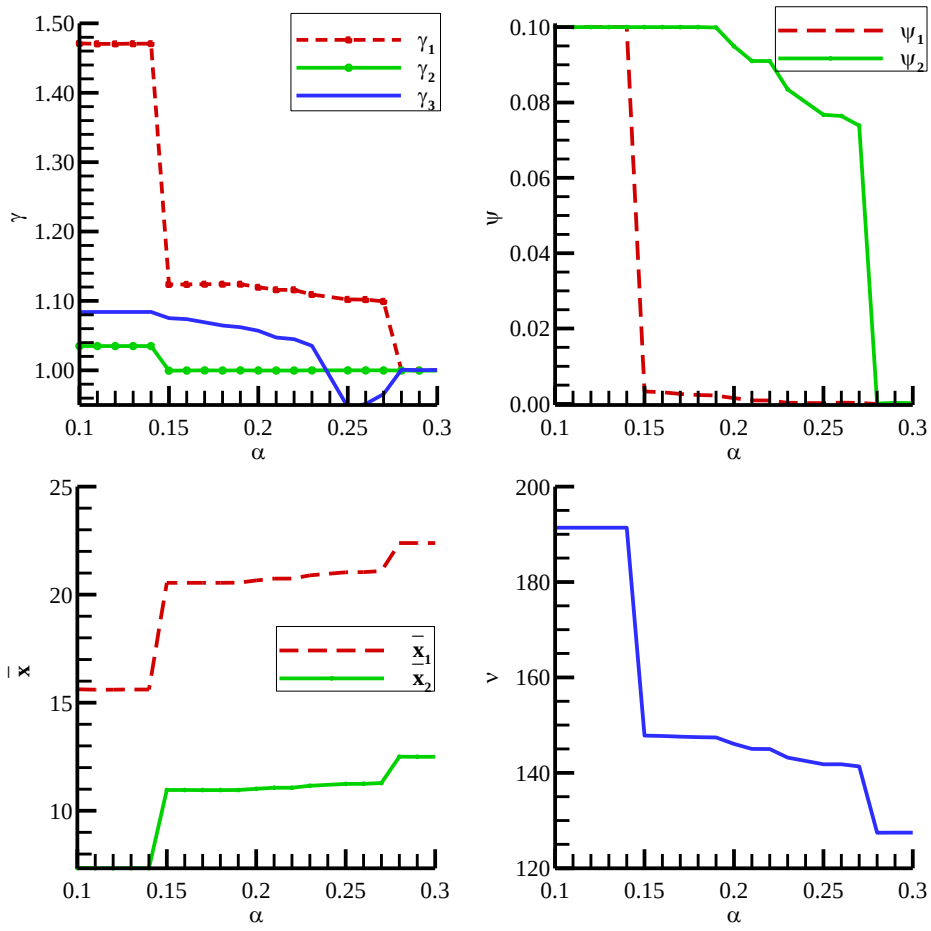

Fig.8 The optimal solution with different α for the mathematical example

Since α is less than 1.0, for increasing α, the weight of f_{opt} increases, and the weight of f_{rob} decreases. When $0.15<\alpha<0.27$, as α increases, V decreases. Due to the existence of uncertainty, the optimization result V that takes into account the uncertainty distribution has increased relative to that of the deterministic optimization, that is, increasing the safety margin. When a <0.5, the main component that affects the objective function is f_{rob}, and both ψ_1 and ψ_2 take the value of the upper bound 0.1. When $0.15<\alpha<0.19$, as α increases, ψ_1 decreases, and ψ_2 reaches the upper bound. When $0.15<\alpha<0.27$, as α increases, ψ_1 and ψ_2 both decrease. When a> 0.27, the main component that affects the objective function is f_{opt}, and both ψ_1 and ψ_2 take the lower bound. The large value of ψ_1 or ψ_2 indicates that the uncertainty in the output is large, and the method based on the first-order expansion has large errors and correction coefficients.

To further verify the accuracy of the proposed method, the MCS is carried out on the optimal solution with $\alpha=0.15$, $\omega_1=\omega_2=0.5$. The optimal solution, the correction coefficients and the MCS results are given in Table 1. The cumulative distribution function and probability density function of the MCS results are shown in Fig.9 and Fig.10, respectively.

Table 1 Optimal solution with $\alpha=0.15$, $\omega_1=\omega_2=0.5$

Optimal solution	V	ψ_1	ψ_2	$\overline{x}_1$	$\overline{x}_2$
	147.7959	0.0033	0.1000	20.5466	10.9612
Correction coefficients	γ_1	γ_2	γ_3		
	1.1238	0.9995	1.0752		

MCS	$P\{f<v\}$	$P\{g_1<0\}$	$P\{g_2<0\}$		
	0.9800	0.9800	0.9836		

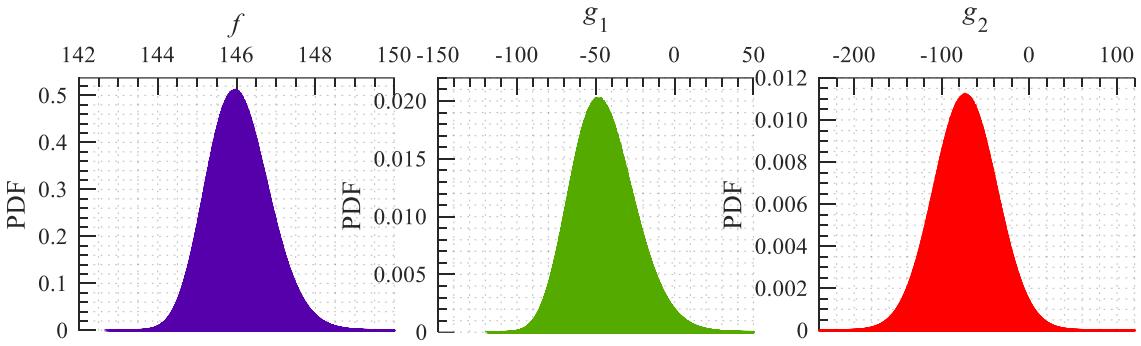

Fig.9 Probability density function of the MCS results

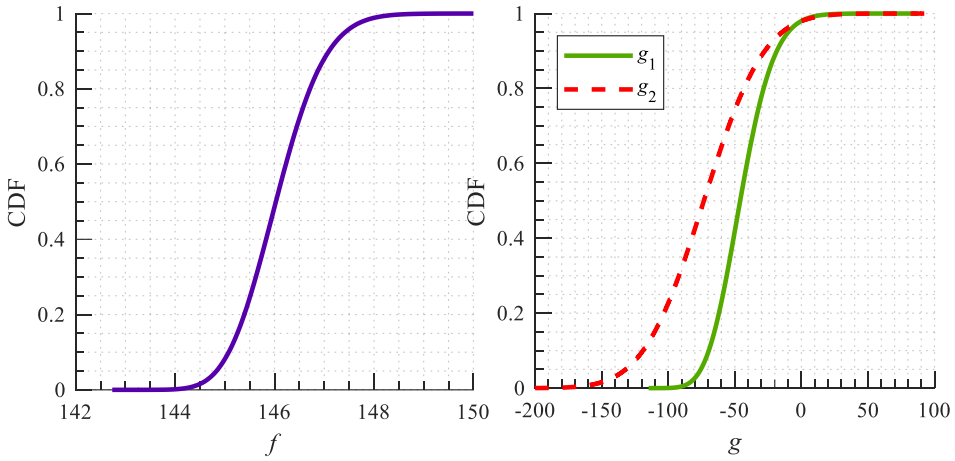

Fig.10 Cumulative distribution function of the MCS results

Due to the quadratic terms in the model function, the results using the first-order method have error. As shown in Fig.9, the probability density functions of the model outputs are not symmetrical to the mean values, which means the outputs are not normally distributed. Therefore, as shown in Table 1, the first-order method needs to be modified, and the correction coefficients γ_1, γ_2, γ_3 are not equal to 1.0. With respect to accuracy, the results illustrate that the framework has high accuracy for quadratic problems, which has been varied by the MCS.

5.2 Cantilever I-beam example

The Cantilever I-beam example is referenced form the literature of uncertainty optimization design (Wang, 2003; Soriano and Dumas, 2012). As shown in Fig.11, $L=200\text{cm}$ is the length of the beam, and the beam is subjected to a vertical load $F_1=600\text{kN}$ and a horizontal load $F_2=50\text{kN}$. The beam section parameters are $u_1=1.0\text{cm}$ and $u_2=2.0\text{cm}$. The elastic modulus of the beam material is $E=2\times10^4\,\text{KN/cm}^2$. The optimization problem is to find the design variables $\{d_1,\ d_2\}$ to minimize the mass subject to the maximum vertical displacement constraint and the maximum stress constraint. The vertical displacement of the beam should be smaller than 1cm and the maximum stress should be smaller than 10kN/cm^2. The deterministic optimization problem of the cantilever I-beam is given as Eq. (33).

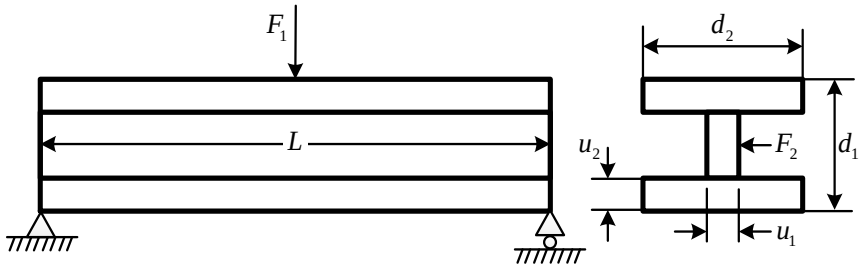

Fig.11 Cantilever I-beam model

$$
\begin{aligned}
&\text{Find} \quad \{d_1, d_2\} \\
&\min \quad f(\mathbf{d},\mathbf{u}) = 2d_2u_2 + u_1(d_1 - 2u_2) \\
&\text{s.t.} \quad g_1(\mathbf{d},\mathbf{u}) = \left(\frac{F_1L^3}{48EI_z}\right) \Big/ D_0 - 1 \\
&\qquad = \frac{5000}{\left(\frac{1}{12}u_1(d_1-2u_2)^3 + \frac{1}{6}d_2u_2^3 + 2d_2u_2\left(\frac{d_1-u_2}{2}\right)^2\right)D_0} - 1 \le 0 \\
&\qquad g_2(\mathbf{x},\mathbf{u}) = \frac{180000d_1}{\left(u_1(d_1-2u_2)^3 + 2d_2u_2\left[4u_2^2 + 3d_1(d_1-2u_2)\right]\right)R} \\
&\qquad + \frac{15000d_2}{\left((d_1-2u_2)u_1^3 + 2u_2d_2^3\right)R} - 1 \le 0 \\
&\qquad 10.0\text{cm} \le d_1 \le 80.0\text{cm}, 10.0\text{cm} \le d_2 \le 50.0\text{cm} \\
&\text{where} \quad u_1 = 1.0,\ u_2 = 2.0,\ R = 16\ \text{kN/cm}^2,\ D_0 = 0.1\text{cm}
\end{aligned}
\tag{33}
$$

The optimal solution for the deterministic optimization problem is $d_1 = 57.3031, d_2 = 24.5655$, and the objective value is $f = 151.5652$.

The uncertainty optimization problem with uncertainty allocation is formulated as Eq. (34).

$$
\begin{aligned}
&\text{find} \quad \{d_1, d_2, \nu, \psi_1, \psi_2\} \\
&\min \quad J = \alpha f_{\text{opt}} + (\alpha - 1) f_{\text{rob}} \\
&\text{s.t.} \quad \mathrm{P}\{g_j(d_1,d_2) \le 0\} \ge 0.98,\ j = 1,2 \\
&\qquad \mathrm{P}\{f(d_1,d_2) \le \nu\} \ge 0.98 \\
&\qquad u_{ai} \sim N\left(\bar{u}_{ai},\ \sigma_{u_{ai}}{}^2\right),\ \psi_i = u_{x_{ai}} / \bar{u}_{ai},\ i = 1,2 \\
&\qquad 10.0\text{cm} \le d_1 \le 80.0\text{cm}, 10.0\text{cm} \le d_2 \le 50.0\text{cm} \\
&\text{where} \quad f_{\text{opt}} = \nu/\beta - 1, \mathrm{f}_{\text{rob}} = \sum \omega_i \psi_i \\
&\qquad \bar{u}_{a1} = 1.0,\ \bar{u}_{a2} = 2.0,\ R = 16\ \text{kN/cm}^2,\ D_0 = 0.1\text{cm}
\end{aligned}
\tag{34}
$$

According to the proposed framework in Fig.7, the uncertainty optimization problem of the cantilever I-beam problem based on the modified first-order approximation method is as expressed in equation Eq. (32).

$$
\begin{aligned}
&\text{Find} \quad \{d_1, d_2, \nu, \psi_1, \psi_2\} \\
&\min \quad J = \alpha f_{\text{opt}} + (\alpha - 1.0) f_{\text{rob}} \\
&\text{s.t.} \quad \mathrm{g}_j(\mathbf{d}, \mathbf{u}) + \gamma_j \Phi^{-1}(0.98)\left(\sum_{i=1}^{2}\left|\frac{\partial \mathrm{g}_j}{\partial u_{ai}}\psi_i \bar{u}_{ai}\right|\right) \le 0,\ j = 1,2 \\
&\qquad f(\mathbf{d}, \mathbf{u}) + \gamma_3 \Phi^{-1}(0.98)\left(\sum_{i=1}^{2}\left|\frac{\partial f}{\partial u_{ai}}\psi_i \bar{u}_{ai}\right|\right) - \nu \le 0 \qquad (35) \\
&\qquad 10.0^{-5} \le \psi_i \le 0.1, i = 1,2 \\
&\text{where} \quad f_{\text{opt}} = \nu/151.5652 - 1, f_{\text{rob}} = (\omega_1\psi_1 + \omega_2\psi_2) \\
&\qquad \bar{u}_{a1} = 1.0,\ \bar{u}_{a2} = 2.0 \\
&\qquad \omega_1 + \omega_2 = 1.0
\end{aligned}
$$

where, the correction coefficients γ_1, γ_2 and γ_3 are solved by using the dimensional adaptive polynomial chaos expansion method as shown in Eq. (26). Since $\omega_1 + \omega_2 = 1.0$, the optimal solutions and correction coefficients with different α and ω_1 are given in Table 2.

Table 2 The optimal solutions and correction coefficients

α	ω_1	γ_1	γ_2	γ_3	ψ_1	ψ_2	d_1	d_2	ν
0.1	0.5	1.2164	1.2383	0.9972	0.0998	0.1000	26.9204	63.5855	191.7136
0.2	0.4	1.2162	1.2382	0.9981	0.0998	0.1000	26.6876	64.5728	191.7345
0.2	0.5	1.1193	1.1226	1.0025	0.0550	0.1000	26.3590	58.3005	175.7602
0.2	0.6	1.0704	1.0708	1.0045	0.0301	0.0999	26.2454	55.2928	168.5683
0.3	0.4	1.0595	1.0541	1.0052	0.0209	0.1000	26.1876	54.3784	166.3983
0.3	0.5	1.0448	1.0449	1.0017	0.0149	0.1000	26.1062	53.9887	165.1454
0.3	0.6	1.0392	1.0319	1.0004	0.0099	0.0999	26.1346	53.4001	164.2812
0.4	0.5	1.0123	1.0134	1.0011	0.0025	0.0293	25.0554	55.9230	155.3105
0.5	0.5	1.0084	1.0092	1.0074	1.15E-05	4.19E-05	24.5762	57.2594	151.5693

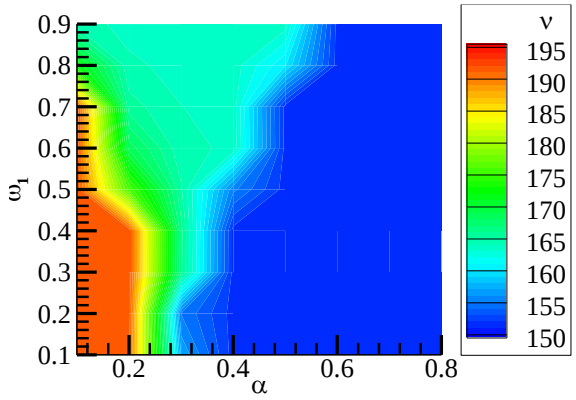

Fig.12 The optimal solution ν according to α and ω_1

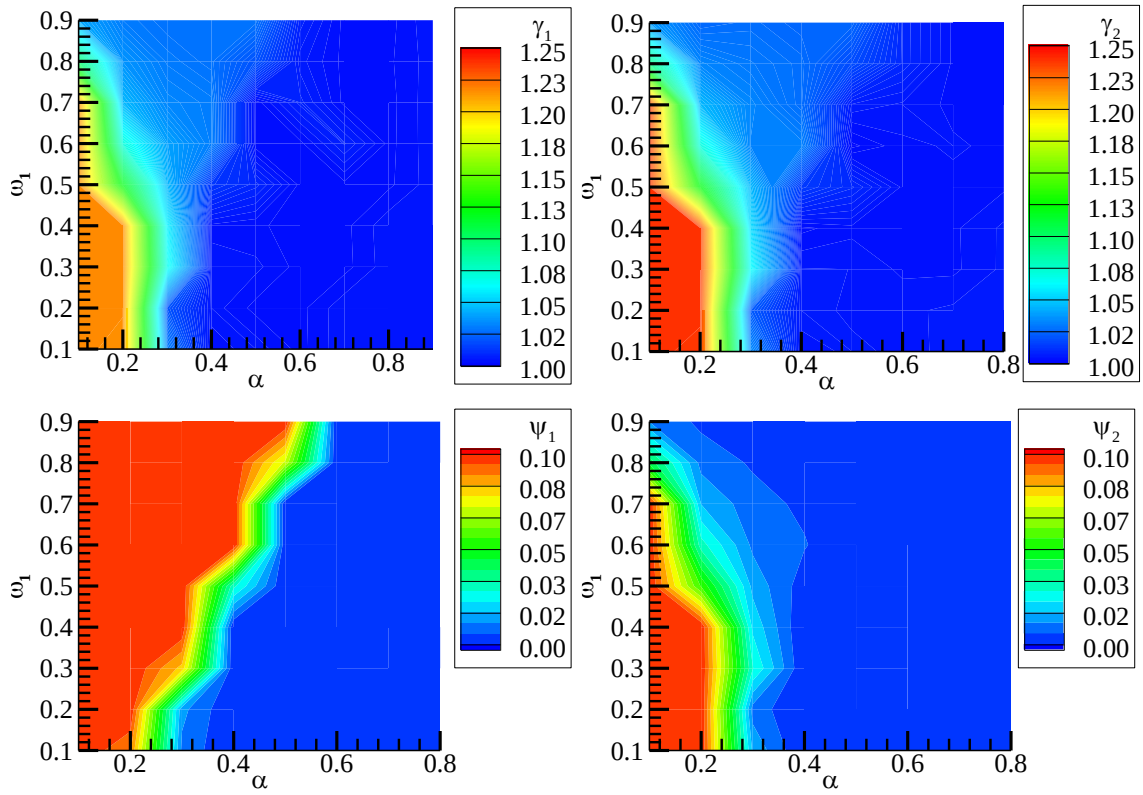

Fig.13 γ_1 , γ_2 , ψ_1 and ψ_2 of optimal solutions according to α and ω_1

When $\alpha = 0.1, 0.2, 0.3, 0.4, 0.5$, the correction coefficients and optimal solutions for different ω_1 are given in Table 2. With the same α , as ω_1 increases, ψ_1 increases, and ψ_2 decreases when it is lower than the upper bound. With the same ω_1 , as α increases, the weight of f_{rob} decreases, the weight of f_{opt} increases, and V decreases until it approaches the objective value of the deterministic optimal solution. For example, the uncertainty allocation parameters ψ_1 and ψ_2 are close to 0, and (d_1, d_2) is close to the optimal solution of the deterministic optimization. The comprehensive trend of the correction coefficient and uncertainty allocation parameters are given in Fig.12 and Fig.13.

According to the physical characteristics of the problem, it is known that when the uncertainty allocation parameters increase, it is necessary to increase the structural strength safety margin to compensate the effect of the uncertainty. To increase the structural safety margin, the structural mass needs to increase. Therefore, as α increases, the weight of f_{rob} decreases, the uncertainty allocation parameters becomes smaller as well, then the corresponding uncertainty becomes smaller, and the required safety margin decreases. Therefore, the optimization process is consistent with the physical characteristics, which verifies the effectiveness of the proposed method.

5.3 **Ten-Bar Truss example**

The ten-bar truss example is referenced from the literature (Au et al. 2003; Jiang et al. 2012; Kang and Luo 2010) . As shown in Fig.14, the lengths of the horizontal and vertical bars are both $L = 360\ \text{in}(9.144\ \text{m})$. The optimization problem of the ten-bar truss is to minimize the structural mass under the stress and displacement constraints. The design variables are the cross-sectional area $A_i, i = 1, 2, \ldots, 10$ of the bars, and the lower bounds of the cross-sectional areas of each bar are all 0.1. The material density is $\rho = 0.1\ \text{lb/in}^3\left(2768\,\text{kg/m}^3\right)$ and the elastic modulus is $E = 10^4$ ksi （68947.57 MPa） . The maximum allowable stress of each bar is the same under tension and compression. The allowable stress of bar ⑨ is 75 ksi (517.11 MPa), and the allowable stress of

other bars is 25 ksi (172.37 MPa). The node 4 subjects to a vertical load F_1, and node 2 subjects to a vertical load F_2 and a horizontal load F_3. The loads are set as $F_1 = F_2 = 444.8\text{kN}(100\text{kip})$ and $F_3 = 0$ according to the literature (Elishakoff et al. 1994; Kang and Luo 2010).

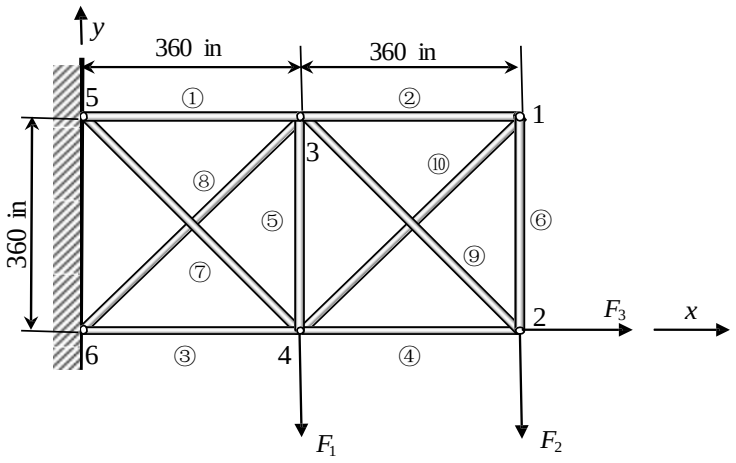

Fig.14 The ten-bar truss model

The system satisfies the set of following equilibrium and compatibility equations (Elishakoff et al. 1994; Hu 2014; Jiang et al. 2012). By solving the balance and compatibility equations, the axial forces $N_i, i = 1, 2, \ldots, 10$ are computed by Eq. (36) .

$$
\begin{aligned}
&N_1 = F_2 - \frac{\sqrt{2}}{2} N_8 && N_2 = -\frac{\sqrt{2}}{2} N_{10} \\
&N_3 = -F_1 - 2F_2 + F_3 - \frac{\sqrt{2}}{2} N_8 && N_4 = -F_2 + F_3 - \frac{\sqrt{2}}{2} N_{10} \\
&N_5 = -F_2 - \frac{\sqrt{2}}{2} N_8 - \frac{\sqrt{2}}{2} N_{10} && N_6 = -\frac{\sqrt{2}}{2} N_{10} \\
&N_7 = \sqrt{2}(F_1 + F_2) + N_8 && N_8 = \frac{a_{22} b_1 - a_{12} b_2}{a_{11} a_{22} - a_{12} a_{21}} \\
&N_9 = \sqrt{2} F_2 + N_{10} && N_{10} = \frac{a_{11} b_2 - a_{21} b_1}{a_{11} a_{22} - a_{12} a_{21}}
\end{aligned}
\quad , \tag{36}
$$

where,

$$
\begin{aligned}
a_{11} &= \left(\frac{1}{A_1} + \frac{1}{A_3} + \frac{1}{A_5} + \frac{2\sqrt{2}}{A_7} + \frac{2\sqrt{2}}{A_8}\right) \frac{L}{2E} \\
a_{21} &= a_{12} = \frac{L}{2A_5 E} \\
a_{22} &= \left(\frac{1}{A_2} + \frac{1}{A_4} + \frac{1}{A_6} + \frac{2\sqrt{2}}{A_9} + \frac{2\sqrt{2}}{A_{10}}\right) \frac{L}{2E} \\
b_1 &= \left(\frac{F_2}{A_1} - \frac{F_1 + 2F_2 - F_3}{A_3} - \frac{F_2}{A_5} - \frac{2\sqrt{2}(F_1 + F_2)}{A_7}\right) \frac{\sqrt{2} L}{2E} \\
b_2 &= \left(\frac{\sqrt{2}(F_3 - F_2)}{A_4} - \frac{\sqrt{2} F_2}{A_5} - \frac{4F_2}{A_9}\right) \frac{L}{2E}
\end{aligned}
\quad , \tag{37}
$$

With the axial forces, the vertical displacement of node 2 can be solved by Eq. (38).

$$D_y = \left(\sum_{i=1}^{6} \frac{N_i^0 N_i}{A_i} + \sqrt{2} \sum_{i=7}^{10} \frac{N_i^0 N_i}{A_i} \right) \frac{L}{E} , \tag{38}$$

where $N_i^0, i = 1, 2, \ldots, 10$ are the axial forces obtained assuming $F_1 = F_3 = 0$ and $F_2 = 1$.

The deterministic optimization problem of minimizing the mass of ten-bar truss is given as Eq. (39).

$$\begin{aligned}
&\text{Find} \quad \mathbf{A} = \{A_i, i = 1, 2, \ldots, 10\} \\
&\min \quad f(\mathbf{A}) = \rho L \left(\sum_{i=1}^{6} A_i + \sqrt{2} \sum_{i=7}^{10} A_i \right) \\
&s.t. \quad g_1(\mathbf{A}) = \max \left\{ \frac{|N_1/A_1|}{25}, \frac{|N_2/A_2|}{25}, \ldots, \frac{|N_8/A_8|}{25}, \frac{|N_9/A_9|}{75}, \frac{|N_{10}/A_{10}|}{25} \right\} \\
&\qquad -1.0,, 0 \\
&\qquad g_2(\mathbf{A}) = D_y - 2 \le 0 \\
&\qquad 0.1 \le A_i \le 50.0, i = 1, 2, \ldots, 10
\end{aligned} \tag{39}$$

The optimal solution of the deterministic optimization is given in Table 3

Table 3 The deterministic optimization results

The cross-section area/ in^2	A_1	30.1222	A_6	0.1000
	A_2	0.1000	A_7	7.4195
	A_3	22.9286	A_8	20.7463
	A_4	15.3957	A_9	21.7755
	A_5	0.1000	A_{10}	0.1000
The mass/lb	f	5022.57		

As shown in the table, due to the loads' characteristics, the cross-section areas of bar ②, ⑤, ⑥, and ⑩ of the deterministic optimization are the lower bounds. Thus, the main load-bearing bars are ①, ③, ④, ⑦, ⑧ and ⑩. Therefore, for the objective function and constraints, the main influencing variables are A_1, A_3, A_4, A_7, A_8 and A_9.

The uncertainty optimization problem with uncertainty allocation is formulated as Eq. (40).

$$\begin{aligned}
&\text{find} \quad \left\{ \bar{A}_1, \bar{A}_2, \ldots, \bar{A}_{10}, \nu, \psi_1, \psi_2, \ldots, \psi_{10} \right\} \\
&\min \quad J = \alpha f_{\text{opt}} + (\alpha - 1) f_{\text{rob}} \\
&\text{s.t.} \quad \mathrm{P}\left\{ g_j(\mathbf{A}) \le 0 \right\} \ge 0.98, \ j = 1,2 \\
&\qquad \mathrm{P}\left\{ f(\mathbf{A}) - \nu \le 0 \right\} \ge 0.98 \\
&\qquad A_i \sim N\left(\bar{A}_i, \ \sigma_{A_i}^{\ 2} \right), \ \psi_i = \bar{A} / \sigma_{A_i} \\
&\qquad 0.1 \le \bar{A}_i \le 50.0, 10^{-5} \le \psi_i \le 0.1, \ i = 1,2, \ldots, 10 \\
&\text{where} \quad f_{\text{opt}} = \nu / 5022.57 - 1, \mathrm{f}_{\text{rob}} = \sum \omega_i \psi_i \ , \\
&\qquad \omega_i = 0.1, \ i = 1,2, \ldots, 10
\end{aligned} \tag{40}$$

According to the proposed framework in Fig.7, the uncertainty optimization problem of the ten-bar truss optimization problem based on the modified first-order approximation method is ~~as expressed in equation Eq. (32).~~

$$
\begin{aligned}
&\text{find} \quad \left\{\bar{A}_1, \bar{A}_2, \ldots, \bar{A}_{10}, \nu, \psi_1, \psi_2, \ldots, \psi_{10}\right\} \\
&\min \quad J=\alpha f_{\text{opt}}+(\alpha-1) f_{\text{rob}} \\
&\text{s.t.} \quad \mathrm{g}_j(\mathbf{A})+\gamma_j \Phi^{-1}(0.98)\left(\sum_{i=1}^{2}\left|\frac{\partial \mathrm{g}_j}{\partial A_i} \psi_i \bar{A}_i\right|\right) \leq 0, \quad j=1,2 \\
&\qquad f(\mathbf{A})+\gamma_3 \Phi^{-1}(0.98)\left(\sum_{i=1}^{2}\left|\frac{\partial f}{\partial A_i} \psi_i \bar{A}_i\right|\right)-\nu \leq 0 \qquad (41) \\
&\qquad A_i \sim N\left(\bar{A}_i, \ \sigma_{A_i}{}^2\right), \quad \psi_i=\bar{A} / \sigma_{A_i} \\
&\qquad 0.1 \leq \bar{A}_i \leq 50.0, 10^{-5} \leq \psi_i \leq 0.1, \quad i=1,2, \ldots, 10 \\
&\text{where} \quad f_{\text{opt}}=\nu / 5022.57-1, \mathrm{f}_{\text{rob}}=\sum \omega_i \psi_i \ , \\
&\qquad \omega_i=0.1, \quad i=1,2, \ldots, 10
\end{aligned}
$$

where, the modified coefficients γ_1 , γ_2 and γ_3 are solved by the dimensional adaptive polynomial chaos method, as given in Eq. (26). Fig.15 shows the correction coefficients and optimal solutions with different α . Since ②, ⑤, ⑥, and ⑩ bars do not influence the stress constraint and displacement constraint, the cross-section areas A_2 , A_5 , A_6 and A_{10} of the optimization result are the lower bounds, and the corresponding uncertainty allocation parameters ψ_2 , ψ_5 , ψ_6 and ψ_{10} are the upper bounds.

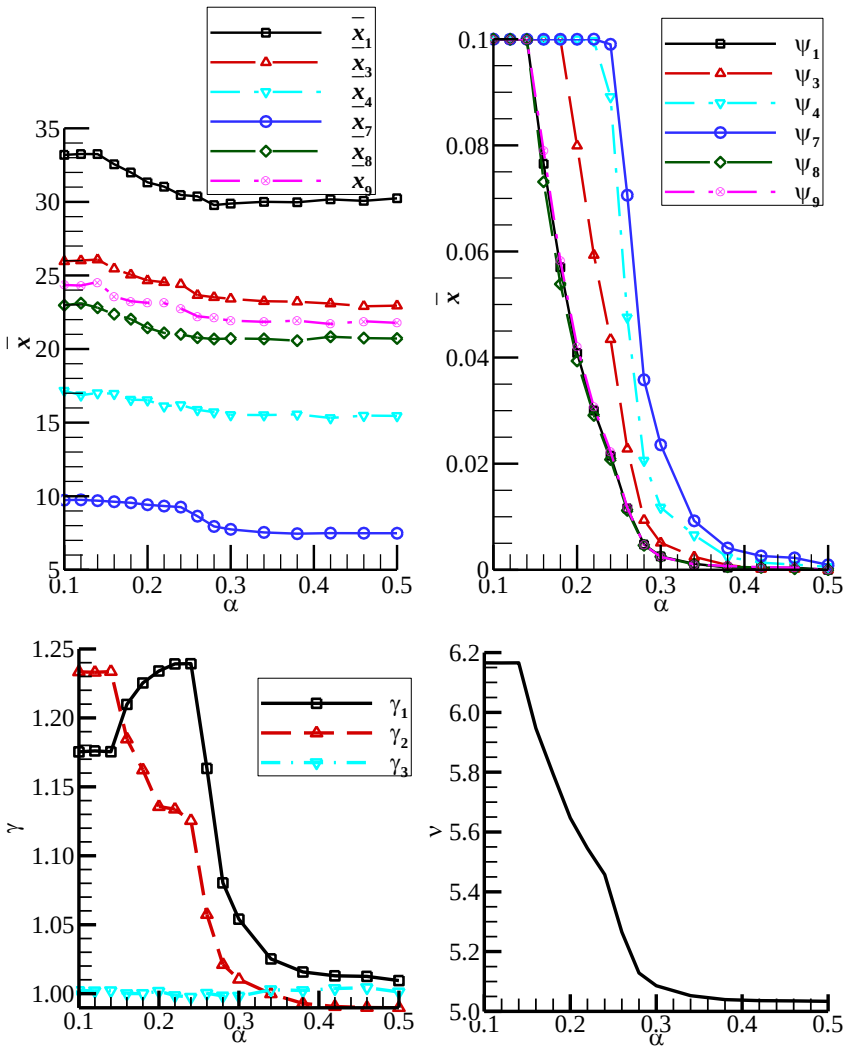

Fig.15 The optimal solution with different α for the ten-bar truss example

Since the mass function is a linear combination of a series of normal distribution variables, the first-order linear method can accurately analyze the uncertainty solution, and the correction coefficient γ_3 is approximately equal to 1.0. When α increases, the weight of f_{rob} decreases and the weight of f_{opt} increases. When $\psi_i \le 0.1$, as α increases, the uncertainty allocation parameters decreases, the cross-sectional areas of the bars decrease, and the mass decreases. It shows that for the larger uncertainty solution, to counteract the influence of uncertainty, the cross-sectional area of each bar increases to enlarge the safety margin, and the corresponding truss mass increases. The optimization results are consistent with the physical properties. The example verifies the effectiveness of the proposed framework on the problem of multiple variables.

6 Conclusion

A sequence optimization framework is proposed to solve the simultaneous design variables selection and probability uncertainty allocation problem. The problem model is constructed by introducing the budget of controlling the uncertainty magnitude to the reliability-based optimization. The input uncertainty parameters are model as the normally distributed parameters. The uncertainty magnitude that needs to be allocated is the standard deviation. The smaller the standard deviation of the input uncertainty parameter, the higher the budget and reliability. The objective is constructed as a combination of the system performance and the budget using the weight coefficient method. Taylor-based method is adopted to translate the probability constraint into the deterministic constraint. To guarantee the accuracy of the framework, the PCE method is adopted to modify the Taylor-based method sequentially. The mathematical example, the cantilever I-beam example and the ten-bar truss example validate the accuracy and effectiveness of the proposed framework. In the mathematical example, the optimization results are validated by the MCS, which shows high accuracy. The optimization results are consistent with the physical characteristic in the cantilever I-beam example, which shows the effectiveness in solving the structure design problem. In the ten-bar truss example, the problem has ten design variables and ten uncertainty allocation parameters, which verify the effectiveness of solving multidimensional problems.

Acknowledgment

The present work was partially supported by the National Defense Fundamental Research Funds of China (Grant No. JCKY2016204B102), and China Civil Aerospace Program (Grant No. D010403), the Natural National Science Foundation of China (Grant No. 51505385, 11502209).

References

Aoues Y, Chateauneuf A (2010) Benchmark study of numerical methods for reliability-based design optimization Struct Multidiscip O 41:277-294 doi:10.1007/s00158-009-0412-2

Au FTK, Cheng YS, Tham LG, Zeng GW (2003) Robust design of structures using convex models Computers and Structures 81:2611-2619 doi:10.1016/S0045-7949(03)00322-5

Beyer HG, Sendhoff B (2007) Robust optimization - A comprehensive survey Computer Methods in Applied Mechanics and Engineering 196:3190-3218 doi:10.1016/j.cma.2007.03.003

Chase KW, Greenwood WH, Loosli BG, Hauglund LF (1990) Least Cost Tolerance Allocation for Mechanical Assemblies with Automated Process Selection MANUFACTURING REVIEW 3:49-59

Chen TC, Fischer GW (2000) A GA-based search method for the tolerance allocation problem Artificial Intelligence in Engineering 14:133-141 doi:10.1016/s0954-1810(00)00006-6

Da Ronch A, Ghoreyshi M, Badcock KJ (2011) On the generation of flight dynamics aerodynamic tables by computational fluid dynamics Prog Aeosp Sci 47:597-620 doi:10.1016/j.paerosci.2011.09.001

Du X, Chen W (2004) Sequential Optimization and Reliability Assessment Method for Efficient Probabilistic Design J Mech Design 126:225-233 doi:10.1115/1.1649968

Dupinet E, Balazinski M, Czogala E (1996) Tolerance allocation based on fuzzy logic and simulated annealing J Intell Manuf 7:487-497 doi:10.1007/bf00122838

Elishakoff I, Haftka RT, Fang J (1994) Structural design under bounded uncertainty—Optimization with anti-optimization Comput Struct 53:1401-1405 doi:https://doi.org/10.1016/0045-7949(94)90405-7
Geetha K, Ravindran D, Kumar MS, Islam MN (2013) Multi-objective optimization for optimum tolerance synthesis with process and machine selection using a genetic algorithm Int J Adv Manuf Tech 67:2439-2457 doi:10.1007/s00170-012-4662-6
Hu Z. (2014). Probabilistic engineering analysis and design under time-dependent uncertainty., Missouri University of Science and Technology,
Huang YM, Shiau CS (2006) Optimal tolerance allocation for a sliding vane compressor J Mech Design 128:98-107 doi:10.1115/1.2114893
Hung T, Chan K (2013) Multi-objective design and tolerance allocation for single- and multi-level systems J Intell Manuf 24:559-573 doi:10.1007/s10845-011-0608-3
Jiang C, Lu GY, Han X, Liu LX (2012) A new reliability analysis method for uncertain structures with random and interval variables Int J Mech Mater Des 8:169-182 doi:10.1007/s10999-012-9184-8
Jiang C, Xie HC, Zhang ZG, Han X (2014) A new interval optimization method considering tolerance design Eng Optimiz 47:1637-1650 doi:10.1080/0305215x.2014.982632
Joseph GD (2016) Multiobjective Formulation for Simultaneous Design and Selection of an Uncertainty Set Aiaa J 54:1742-1750 doi:10.2514/1.J054529
Joseph GD (2017) Variations in the application of a budget of uncertainty optimization approach Struct Multidiscip O 55:77-89 doi:10.1007/s00158-016-1473-7
Kang Z, Luo Y (2010) Reliability-based structural optimization with probability and convex set hybrid models Struct Multidiscip O 42:89-102 doi:10.1007/s00158-009-0461-6
Keshavarzzadeh V, Meidani H, Tortorelli DA (2016) Gradient based design optimization under uncertainty via stochastic expansion methods Computer Methods in Applied Mechanics and Engineering 306:47-76 doi:10.1016/j.cma.2016.03.046
Keshtegar B, Hao P (2016) A Hybrid Loop Approach Using the Sufficient Descent Condition for Accurate, Robust, and Efficient Reliability-Based Design Optimization Journal of Mechanical Design 138:121401-121401-121411 doi:10.1115/1.4034173
Keshtegar B, Hao P (2017) A hybrid self-adjusted mean value method for reliability-based design optimization using sufficient descent condition Applied Mathematical Modelling 41:257-270 doi:https://doi.org/10.1016/j.apm.2016.08.031
Keshtegar B, Hao P (2018) Enhanced single-loop method for efficient reliability-based design optimization with complex constraints Structural and Multidisciplinary Optimization 57:1731-1747 doi:10.1007/s00158-017-1842-x
Kusiak A, Feng C (1995) Deterministic tolerance synthesis: a comparative study Comput Aided Design 27:759-768 doi:10.1016/0010-4485(94)00028-C
Li J (2016) Probability density evolution method: Background, significance and recent developments Probabilistic Engineering Mechanics 44:111-117 doi:https://doi.org/10.1016/j.probengmech.2015.09.013
Li X, Gong C, Gu L, Jing Z, Fang H, Gao R (2019) A reliability-based optimization method using sequential surrogate model and Monte Carlo simulation Struct Multidiscip O 59:439-460 doi:10.1007/s00158-018-2075-3
Liu Y, Jeong HK, Collette M (2016) Efficient optimization of reliability-constrained structural design problems including interval uncertainty Comput Struct 177:1-11 doi:10.1016/j.compstruc.2016.08.004
Lopez RH, Beck AT (2012) Reliability-Based Design Optimization Strategies Based on FORM: A Review J Braz Soc Mech Sci 34:506-514
Luo Y, Wu X, Zhou M, Wang MY (2015) Simultaneous parameter and tolerance optimization of structures via probability-interval mixed reliability model Struct Multidiscip O 51:705-719 doi:10.1007/s00158-014-1167-y
Meng Z, Hao P, Li G, Wang B, Zhang K (2015) Non-probabilistic reliability-based design optimization of stiffened shells under buckling constraint Thin Wall Struct 94:325-333 doi:10.1016/j.tws.2015.04.031
Meng Z, Li G, Wang BP, Hao P (2015) A hybrid chaos control approach of the performance measure functions for reliability-based design optimization Comput Struct 146:32-43 doi:10.1016/j.compstruc.2014.08.011
Meng Z, Zhou H, Li G, Yang D (2016) A decoupled approach for non-probabilistic reliability-based design optimization Computers & Structures 175:65-73

doi:https://doi.org/10.1016/j.compstruc.2016.06.008
Padulo M, Campobasso MS, Guenov MD (2011) Novel Uncertainty Propagation Method for Robust Aerodynamic Design Aiaa Journal 49:530-543 doi:10.2514/1.J050448
Papadimitriou DI, Papadimitriou C (2016) Aerodynamic shape optimization for minimum robust drag and lift reliability constraint Aerospace Science and Technology 55:24-33 doi:10.1016/j.ast.2016.05.005
Park C, Kim NH, Haftka RT (2015) The effect of ignoring dependence between failure modes on evaluating system reliability Structural and Multidisciplinary Optimization 52:251-268 doi:10.1007/s00158-015-1239-7
Prabhaharan G, Asokan P, Ramesh P, Rajendran S (2004) Genetic-algorithm-based optimal tolerance allocation using a least-cost model Int J Adv Manuf Tech 24:647-660 doi:10.1007/s00170-003-1606-1
Rao SS, Wu A (2005) Optimum tolerance allocation in mechanical assemblies using an interval method Eng Optimiz 37:237-257 doi:10.1080/0305215512331328240
Schillings C (2010) Optimal Aerodynamic Design under Uncertainties. Universität Trier
Schillings C, Schulz V (2015) On the influence of robustness measures on shape optimization with stochastic uncertainties Optimization and Engineering 16:347-386 doi:10.1007/s11081-014-9251-0
Shahraki AF, Noorossana R (2014) Reliability-based robust design optimization: A general methodology using genetic algorithm Comput Ind Eng 74:199-207 doi:10.1016/j.cie.2014.05.013
Silva M, Tortorelli DA, Norato JA, Ha C, Bae H (2010) Component and system reliability-based topology optimization using a single-loop method Struct Multidiscip O 41:87-106 doi:10.1007/s00158-009-0401-5
Smoljak SA (1963) Quadrature and interpolation formulas for tensor products of certain classes of functions Dokl Akad Nauk SSSR 148:1042-1045 doi:http://www.mathnet.ru/php/archive.phtml?wshow=paper&jrnid=dan&paperid=27586&option_lang=eng (online available)
Torii AJ, Lopez RH, Biondini F (2012) An approach to reliability-based shape and topology optimization of truss structures Eng Optimiz 44:37-53 doi:10.1080/0305215X.2011.558578
Torii AJ, Lopez RH, Miguel LFF (2017) A gradient-based polynomial chaos approach for risk and reliability-based design optimization Journal of the Brazilian Society of Mechanical Sciences and Engineering 39:2905-2915 doi:10.1007/s40430-017-0815-8
Valdebenito MA, Schueller GI (2010) A survey on approaches for reliability-based optimization Struct Multidiscip O 42:645-663 doi:10.1007/s00158-010-0518-6
Wu F, Dantan J, Etienne A, Siadat A, Martin P (2009) Improved algorithm for tolerance allocation based on Monte Carlo simulation and discrete optimization Comput Ind Eng 56:1402-1413 doi:10.1016/j.cie.2008.09.005
Wu X, Zhang W, Song S (2018) Robust aerodynamic shape design based on an adaptive stochastic optimization framework Structural and Multidisciplinary Optimization 57:639-651 doi:10.1007/s00158-017-1766-5
Xiu DB, Karniadakis GE (2002) The Wiener-Askey polynomial chaos for stochastic differential equations Siam Journal on Scientific Computing 24:619-644 doi:10.1137/S1064827501387826
Yang D, Liu L (2014) Reliability analysis of structures with complex limit state functions using probability density evolution method Structural and Multidisciplinary Optimization 50:275-286 doi:10.1007/s00158-014-1048-4
Yi P, Zhu Z, Gong J (2016) An approximate sequential optimization and reliability assessment method for reliability-based design optimization Struct Multidiscip O 54:1367-1378 doi:10.1007/s00158-016-1478-2
Youn BD, Choi KK, Du L (2005) Enriched Performance Measure Approach for Reliability-Based Design Optimization AIAA Journal 43:874-884 doi:10.2514/1.6648
Zhang C, Wang H (1993) Integrated tolerance optimisation with simulated annealing Int J Adv Manuf Tech 8:167-174 doi:10.1007/bf01749907